Kinetics of the Solid-State Carbothermic Reduction of Wessel Manganese Ores

GUVEN AKDOGAN and R. HURMAN ERIC

Reduction of manganese ores from the Wessel mine of South Africa has been investigated in the temperature range 1100 °C to 1350 °C with pure graphite as the reductant under argon atmosphere. The rate and degree of reduction were found to increase with increasing temperature and decreasing particle sizes of both the ore and the graphite. The reduction was found to occur in two stages: (1) The first stage includes the rapid reduction of higher oxides of manganese and iron to MnO and FeO. The rate control appears to be mixed, both inward diffusion of CO and outward diffusion of CO_2 across the porous product layer, and the reaction of carbon monoxide on the pore walls of the oxide phase play important roles. The values of effective CO-CO_2 diffusivities generated by the mathematical model are in the range from 2.15×10^{-5} to 6.17×10^{-5} $cm^2 \cdot s^{-1}$ for different ores at 1300 °C. Apparent activation energies range from 81.3 to 94.6 kJ/kg/mol. (2) The second stage is slower during which MnO and FeO are reduced to mixed carbide of iron and manganese. The chemical reaction between the manganous oxide and carbon dissolved in the metal phase or metal carbide seems to be the rate-controlling process. The rate constant of chemical reaction between MnO and carbide on the surface of the impervious core was found to lie in the range from 1.53×10^{-8} to 1.32×10^{-7} $mol \cdot s^{-1} \cdot cm^{-2}$. Apparent activation energies calculated are in the range from 102.1 to 141.7 kJ/kg/mol.

I. INTRODUCTION

MANGANESE ore production in South Africa is estimated to be the second largest in the world after the former USSR.[1] Manganese ore deposits in South Africa that are situated in the Northern Cape Province include Wessel, Mamatwan, and Hotazel mines. Wessel type is a hydrothermally upgraded, carbonate poor, braunite, hausmannite, bixbyite, and braunite II bearing manganese ore.[2]

Prereduction of manganese ore with carbon could be a promising route to increase cost-effectiveness of ferromanganese production.[3] The prereduced material may then be smelted in an open-arc furnace to produce ferromanganese and slag. It was reported that the energy consumption has dropped from about 3000 kWh/ton FeMn to about 1600 kWh/ton FeMn when prereduced pellets were used instead of ore in the electric furnace.[4]

Most of the investigators who studied the reduction of metal oxides by carbon assumed that the overall rate of reaction was controlled by the reaction between carbon dioxide and carbon at temperatures up to 1000 °C.[5,6,7] At higher temperatures, this reaction (also known as Boudouard reaction) is quite fast, and hence, the rate-controlling step of reduction of metal oxides could be different.[8]

$$CO_2 + C = 2CO \qquad [1]$$

At low temperatures up to 1000 °C to 1050 °C, the rate of Reaction [1] is dependent upon the temperature and is controlled by chemical reaction. At temperatures above 1100 °C, the rate is controlled by diffusion.[9–19] The kinetic studies on the C-CO_2 reaction have not produced a generally accepted value for activation energy for Reaction [1]. The reported activation energies vary from 246.6 to 405.5 kJ/kg/mol.[6,10,15–18] Kor[19] investigated the rate of reduction of Mn_3O_4 to MnO by carbon between 900 °C and 1200 °C and concluded that the overall rate is controlled by the rate of oxidation of carbon in CO_2; although, there is a considerable overlap between pore diffusion control and chemical reaction control for the Boudouard reaction in the range 1000 °C to 1100 °C.[20,21,22] Tereyama and Ikeda[23] reduced MnO with carbon under helium atmosphere in the range 1100 °C to 1200 °C and reported that the overall rate seemed to be controlled by the rate of oxidation of carbon by carbon dioxide.

Rankin and Van Deventer[24] developed a kinetic model for the reduction of MnO by graphite derived on the conclusion that the gasification of graphite was the rate-controlling step in the temperature range 1200 °C to 1425 °C for which an activation energy of 240.4 kJ/kg/mol was calculated. Koursaris *et al.*[25] found that the stages of reduction of Mamatwan ore with carbon in the range between 1200 °C and 1600 °C involve complex mineralogical changes, which includes (1) the breakdown of Braunite and gangue minerals, (2) the reduction of higher manganese oxides to MnO and hematite to metallic iron, and (3) the formation of slag as a result of the reaction between gangue and manganous oxide. They also stated that further reduction of the ore involves the carburization of the metallic phase and the reduction of solid MnO, or MnO dissolved in the slag, by solid carbon or carbon dissolved in the metal. Dewar and See[26] investigated the influence of different carbonaceous reducing agents on the rate of reduction of

GUVEN AKDOGAN, formerly Doctoral Student, Department of Metallurgy and Materials Engineering, University of the Witwatersrand, Johannesburg, is Lecturer with the Mining Engineering Department, Istanbul University, Turkey. R. HURMAN ERIC, Professor in the Chamber of Mines, Chair of Extractive Metallurgy, and Head of Department, is with the Department of Metallurgy and Materials Engineering, University of the Witwatersrand, Johannesburg, WITS 2050, South Africa.

Manuscript submitted December 14, 1993.

Mamatwan manganese ore and concluded that there were no significant differences in the mode of reduction with different reducing agents.

Antonov and Chyfarov[27] found that addition of Fe_2O_3 to a mixture of MnO and carbon under a carbon monoxide atmosphere between 1300 °C and 1380 °C increased the rate of MnO reduction by formation of (Fe, Mn)O, which in turn facilitates the reduction reaction. Tsylev[28] stated that it was possible that the solid-state reduction of manganese and iron oxides proceeds *via* an intermediate reducing agent like Fe_3C. Van Hien and Ryzhonkov[29] found that the presence of FeO lowered the temperature for solid-state reduction of MnO with carbon. Ashin and Rostovchev[30] proposed that over the temperature range from 1310 °C to 1400 °C, the reduction of MnO by carbon occurs *via* carbon dissolved in the liquid manganese product.

Grimsely[31] proposed a two-step process for the reduction of preheated Mamatwan manganese ore between 1000 °C and 1300 °C. The first step includes the reduction of Mn_3O_4 by carbon and carbon monoxide, while the second step involves the reduction of MnO by a carbide. The reduction of preheated ore was faster than that of pure Mn_3O_4 during the second step of the reduction. This was attributed to the presence of iron in the ore that could form an intermediate carbide through which carbon is transported to the reaction interface. During the second, longer step, MnO and $CaMn_2O_4$ (which were formed during the first step) were reduced to carbides by carbon dissolved in the ferromanganese phase.

Misra[32] examined the response of manganese ore pellets to the prereduction by the use of a coke powder under nitrogen in the range 800 °C to 1260 °C and observed that the reaction rate was high at the beginning but slowed down to an asymptotic value as the time proceeded. He calculated an activation energy of 37.4 kJ/kg/mol from the reduction rates for the initial region of the kinetic curves for the reduction to MnO stage and attributed this low activation energy to the indirect reduction by means of carbon packing by which he assumed that the overall rate was controlled by the rate of oxidation of carbon. Eric and Burucu,[33] who investigated the mechanism and kinetics of reduction of the Mamatwan manganese ore with graphite under argon atmosphere between 1100 °C and 1350 °C, proposed a three-stage process. The first stage was between a 0- and 30-pct reduction during which higher manganese oxides and iron oxide were reduced to MnO and FeO for which an apparent activation energy of 61 kJ/kg/mol was calculated and attributed to the gaseous diffusional processes across the porous oxide product layer. The second stage took place between 30- and 70-pct reduction and included the random nucleation of iron, followed by formation of iron-rich Fe-Mn carbides and a silicate phase. During this stage, chemical reaction between oxide phase and gaseous phase was proposed to be the rate-controlling step with an activation energy of 153.3 kJ/kg/mol. During the last stage, which started after 70 pct reduction level, the remaining oxide was reduced by carbon dissolved in the carbide phase. The diffusion of Mn^{2+} ions in the oxide was assumed as the slowest process with an apparent activation energy of 310.4 kJ/kg/mol. On the other hand, there is no information on the reduction and smelting behavior of Wessel manganese ores.

II. EXPERIMENTAL DETAILS

Experiments were conducted by use of a thermogravimetric analyzer (TGA) consisting of a vertical molybdenum-wound resistance furnace with a recrystallized alumina work tube of 50-mm internal diameter. The molybdenum wires were protected from oxidation by cracked anhydrous ammonia atmosphere. Furnace temperature was controlled by a *B*-type thermocouple (Pt-6 pct Rh/Pt-30 pct Rh) suspended in the work tube just above the crucible, which was connected to a Eurotherm thyristor-coupled controller. Sample temperatures were measured by a separate *B*-type thermocouple. The digital electronic balance was placed in a gas-tight perspex box, and the pan of the balance was replaced with an alumina rod and pedestal. The balance case was connected to the furnace work tube, from the bottom by gas-tight flexible rubber bellows. The balance could be moved up and down by a hoisting mechanism. Weight loss measurements during reduction were stored on a personal computer, which was interfaced to the balance. Kinetic curves (reduction percent *vs* time) were plotted by the computer, utilizing data points that were averaged at 1-minute intervals. The ancillary parts of the experimental apparatus included a gas-cleaning train involving a column filled with anhydrous $Mg(ClO_4)_2$ as a desiccant and a tube furnace heated to 500 °C containing copper chips as a deoxidant, flow meters, and a digital temperature display. All throughout the experimental runs, alumina crucibles were used to hold the samples.

Manganese ores designated as WH, W1, and W4 from the Wessel mine in the Kalahari field were supplied by Samancor, the chemical analyses of which are given in Table I. The reducing agent used in the reduction experiments was spectrographically pure graphite, which contained less than 10 parts per million impurities. The graphite particle size was 100 pct—0.044 mm.

Manganese ore and graphite were mixed in the ratio of four parts of ore to one part of graphite (by mass) under acetone in an agate mortar. The wet mixture was poured into a 36-mm-diameter × 56-mm-high alumina

Table I. The Chemical Compositions of Wessel Manganese Ores

Constituents	Percent (by Mass)		
	WH	W1	W4
MgO	0.30	0.20	0.20
Al_2O_3	0.30	0.40	0.30
SiO_2	3.90	3.10	5.51
CaO	4.80	4.80	9.41
$Mn_2O_3^*$	75.09	68.69	50.78
$Fe_2O_3^{**}$	12.86	17.53	27.20
CO_2	0.90	0.70	1.10
H_2O	0.10	0.20	0.20

*Total manganese expressed as Mn_2O_3.
**Total iron expressed as Fe_2O_3.

crucible and was dried in an oven at 105 °C. The crucible was weighed with and without its contents prior to experiments and after completion of reduction runs. The crucible, together with its contents, was placed on the balance pedestal, the rubber bellows was connected to the furnace, and argon purging was started. The crucible, together with the balance, was raised into the hot zone of the furnace by use of the hoisting mechanism under an argon flow rate of 1000 cm^3/min (measured at 25 °C and at atmospheric pressure). Weight loss measurement was started as soon as the sample was raised into the hot zone after zeroing of weight reading on the balance. Experimental runs were allowed to proceed up to 120 minutes, whereupon they were stopped by lowering the balance assembly quickly so that the sample could cool in a flow of argon gas. The checking of the weight of the crucible before and after the reduction on a separate balance proved that the reduction percentages calculated by the computer were correct, and the results were reproducible within 1 pct.

Furthermore, at the end of each of the 20 runs, duplicate runs were conducted at the same conditions with the same charge materials. These runs were also reproducible within 1 pct all throughout the reduction period. In order to ensure that there were no leaks, a carbon blank run was carried out also at the end of each of the 20 runs.

The reduced samples were split into representative portions and were analyzed (1) chemically by X-ray fluorescence of inductively coupled plasma emission spectroscopy, (2) by X-ray diffraction (XRD) for phase identifications, (3) metallographically, and (4) by scanning electron microscopy–energy-dispersive X-ray analysis (SEM-EDAX) for microanalysis of phases.

The data on mass loss were converted to reduction percentage, based on the assumption that the loss in mass of the sample was due to carbon monoxide evolution. The existence of appreciable amount of carbon dioxide is not possible at temperatures above 1000 °C in the presence of carbon. This was further ensured by using excess carbon. The percentage reduction was, therefore, described as

$$R\ \text{pct} = \frac{\text{mass of CO evolved}}{\text{mass of original removable oxygen}} \frac{16}{28} \times 100 \quad [2]$$

Two oxides, Mn_2O_3 and Fe_2O_3, were considered to be reducible under the prevailing conditions. The stoichiometric amount of carbon was calculated, based on the reduction of Mn_2O_3 to Mn_7C_3 and the reduction of Fe_2O_3 to Fe_3C.

III. RESULTS AND DISCUSSION

In the presentation of results and in kinetic calculations, the data gathered on all three ore types, namely, W1, W4, and WH, were used. The behavior of all three ore types are the same, the only differences being small changes in reduction levels due to small differences in their compositions.

A. *Reduction Experiments*

The most significant factor influencing reduction rate and degree was temperature, causing about a threefold increase in reduction degree from 1100 °C to 1350 °C, as illustrated in Figure 1. All the reduction vs time curves showed a marked slowdown in the rate from about 6 minutes of reaction time. This point of change in the slopes of kinetic curves corresponded to approximately a 33-pct reduction at temperatures above 1200 °C. Thus, the reduction proceeded in two stages: a short initial stage during which the rate and degree of reduction were affected slightly by temperature and a second longer stage during which the effect of temperature on the degree of reduction was substantial.

The effect of ore particle size on the rate and degree of reduction was not very pronounced up to approximately a 35-pct reduction. Thereafter, there was a large decrease in reaction rate and extent when ore particle size was increased to between 0.210 and 0.297 mm. The effect of particle size on the reduction rate and degree at 1300 °C is shown in Figure 2, where curve 1 depicts the behavior of a composite sample containing all particle sizes from −0.297 mm downwards.

The particle size of graphite has also influenced the reduction extent and rate. There was a considerable decrease in the reduction rate and amount when the particle size of graphite was increased to between 0.150 and 0.210 mm, as shown in Figure 3. This result is supported by a number of investigations on the reduction of manganese ores and manganese oxide.[23,24,33]

The effect of carbon content over and above the stoichiometric amount had a slight effect: increasing the degree of reduction by about 10 pct when the carbon amount was increased from the stoichiometric requirement to an 8-pct excess. Further increase in the carbon amount had a negligible effect.

The influence of various factors such as the Mn:Fe ratio and Fe_2O_3 and Mn_2O_3 contents on reducibility of Wessel manganese ores at 1300 °C is summarized in

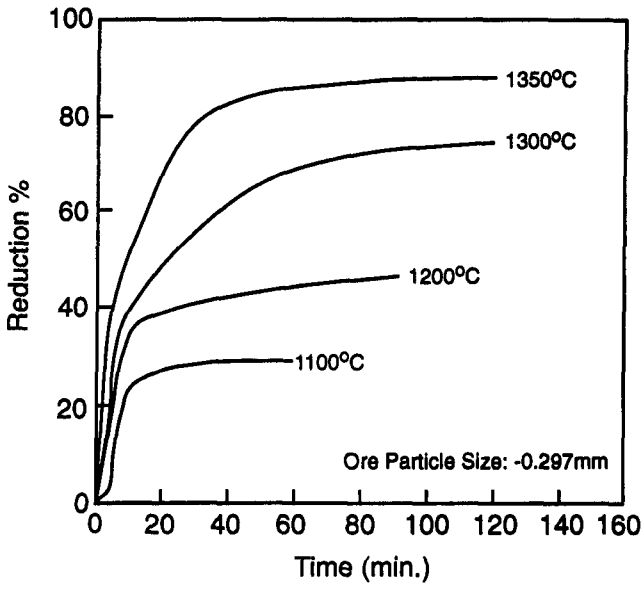

Fig. 1—Effect of temperature on the reduction of WH ore.

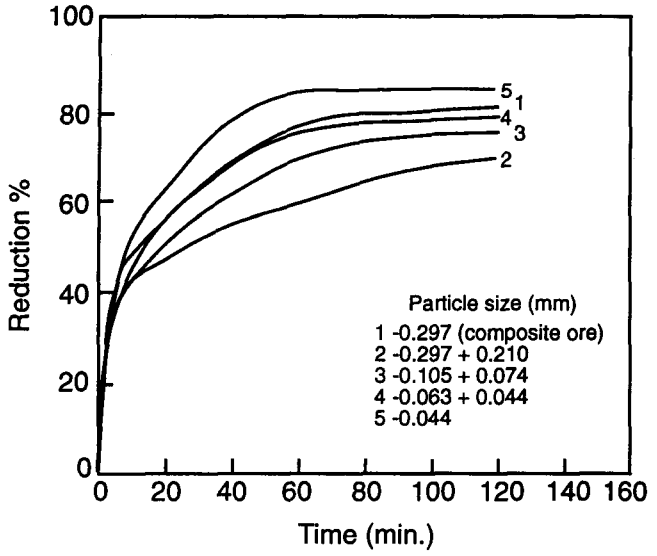

Fig. 2—Effect of particle size on the reduction of W1 ore at 1300 °C.

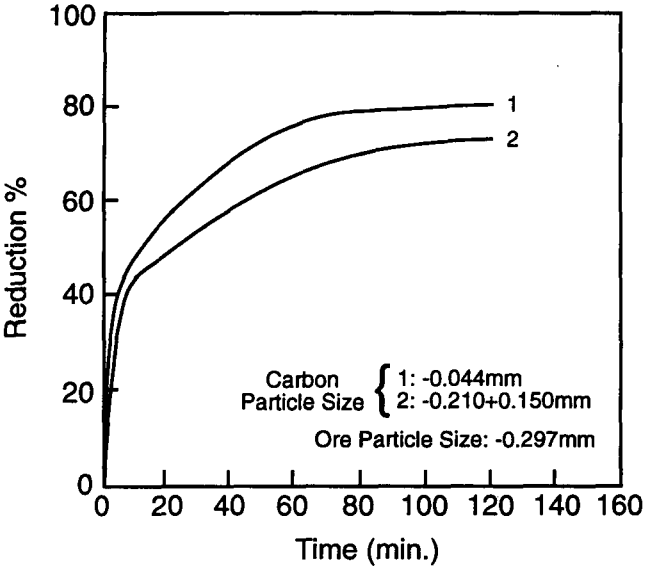

Fig. 3—Effect of carbon particle size on the reduction of W1 ore at 1300 °C.

Table II. The reduction curves of three different manganese samples reduced at 1300 °C are illustrated in Figure 4. The Mn_2O_3 content of the ore samples used in this investigation ranges from 50.78 to 75.09 pct manganese:iron ratios vary from 1.86 to 5.82, while Fe_2O_3 content changes from 12.86 to 27.20 pct. Considering Table II and Figure 4 together, several important factors emerge between the chemical components and reducibility. The most easily reduced ore, W4, had the lowest Mn:Fe ratio and the highest Fe_2O_3. Conversely, the ores that were more difficult to reduce, WH and W1, had higher Mn:Fe ratios and the lower Fe_2O_3 content. This result is in accord with those of Rankin and Van Deventer,[24] Grimsley,[31] and Eric and Burucu.[33]

For the reaction between MnO and carbon to produce metallic manganese, the standard free-energy change does not become negative before 1420 °C is reached. Thus, manganese metal cannot appear in this system before it melts (melting point of manganese is 1244 °C) by which time manganese carbide forms.[34] It is thus apparent that the iron content of the ores accelerated the rate of reduction by formation of an intermediate carbide through which the carbon is transported to the reaction interface.

Figure 5 illustrates the variation in the reduction percentage of W1 ore reacted with only carbon monoxide and with carbon in argon and carbon monoxide atmospheres, respectively, at 1300 °C. The overall degrees of reduction achieved with carbon monoxide only and with carbon in carbon monoxide atmosphere were well below the percentage reduction that was achieved with carbon in argon atmosphere. On the other hand, the rate and amount of reduction with solid carbon in carbon monoxide atmosphere were slightly higher than when only carbon monoxide was used. Reduction curves supported by X-ray and EDAX revealed that the reduction in an atmosphere of carbon monoxide (with or without carbon) proceeded until higher manganese oxides were reduced to MnO and iron oxides to metallic iron. Thus, it is apparent that carbon monoxide plays an important role in the reduction of higher valency manganese oxides

Table II. Effect of the Chemical Components on the Reduction of Wessel Manganese Ores Reduced at 1300 °C for 60 Minutes

Manganese Ore	Mn_2O_3 (Pct)	Fe_2O_3 (Pct)	Mn/Fe Ratio	Reduction (Pct)
WH	75.09	12.86	5.82	68.47
W1	68.69	17.53	3.90	75.85
W4	50.78	27.20	1.86	86.01

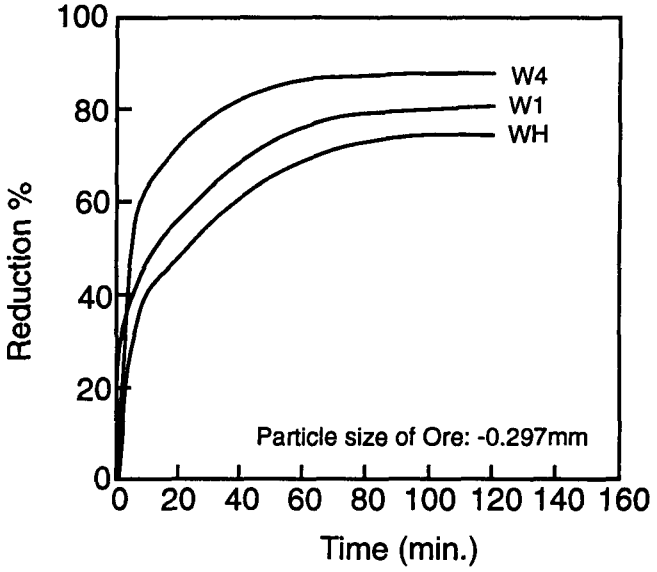

Fig. 4—Reduction *vs* time curves for three different manganese ores reduced at 1300 °C.

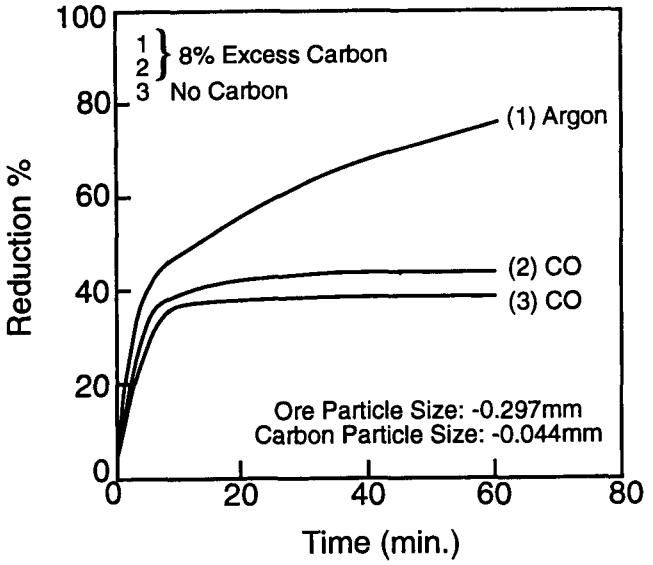

Fig. 5—Effect of carbon monoxide on the reduction of W1 ore at 1300 °C.

to lower oxides. Manganous oxide reduction to metal with carbon monoxide requires very high P_{CO}/P_{CO_2} ratio in the gaseous phase, according to the standard free-energy change of the following reaction:

$$MnO + CO = Mn + CO_2 \quad [3]$$

$$\Delta G^\circ \text{ (kJ/kg/mol)} = +102.3 + 0.01T \ldots \quad (25\ ^\circ\text{C to } 1227\ ^\circ\text{C})$$

$$= +116.7 + 0.01T \ldots \quad (1227\ ^\circ\text{C to } 1727\ ^\circ\text{C})$$

B. *Results of Mineralogical Analysis*

The main phases detected from the diffraction patterns of the original unreduced Wessel manganese ores are shown in Table III, in decreasing order of abundance, as measured from the relative peak intensity on the diffractograms. The compositional changes taking place during the reduction (with excess graphite) at 1300 °C under argon atmosphere are summarized in Table IV. The samples subjected to short reduction times from 2 to 10 minutes contained magnetic phases such as Fe_3O_4, $MnFe_2O_4$, and metallic iron (after 6 minutes). With an increase in retention time, the magnetic phases disappeared, and the major phases that were present were carbides. Manganous oxide was present in all samples that were subjected to reduction times of up to 50 minutes. With a further increase in reduction time, the MnO phase disappeared, and some of it was converted to ferromanganese carbide, while at the same time, the remaining MnO was dissolved in the silicate slag. The silicate slag started to appear from about 20 minutes of reduction time. The specific composition of the silicate phase could not be determined by XRD analysis; however, judging from the green color of the silicate slag, it was decided that some manganese must have been dissolved in it. At 1350 °C, the peaks of manganous oxide showed a slight shift due to the presence of FeO in solid solution. The composition of the silicate slag phase resembled $(Ca, Mn)_2SiO_4$, which shifted toward Ca_2SiO_2 as manganese was removed from it. The presence of α iron in some of the samples was a function of the reduction of the iron-containing oxide minerals in the ores and retention time of the sample at temperature. The Fe_2O_3 component of the ore was rapidly reduced to magnetite and, with an increase in retention time, eventually to metallic iron.

The main carbides that were identified were Fe_7C_3 and Mn_5C_2. The reaction product Mn_5C_2 was also reported by Rankin and Van Deventer.[24] Fe_3C and $Mn_{15}C_4$ carbides were found only in trace amounts. The Fe_7C_3 carbide was probably stabilized by dissolving some manganese.

On the other hand, XRD analysis showed that manganous oxide (MnO) and metallic iron were the major phases detected in samples reduced in the carbon monoxide atmosphere, confirming the results of reduction curves that slowed abruptly after the conversion of higher manganese oxides to MnO and iron oxide to iron metal.

C. *Results of Microscopic Examination*

Energy-dispersive analysis of X-rays was conducted on the same set of samples that were subjected to mineralogical analysis. The results revealed that no metallic phase was formed at reduction times shorter than 6 minutes, and the particle surface (reaction products) was porous, as shown in Figure 6. Reduction without the formation of metallic phase confirmed the reduction of higher manganese and iron oxides to their lower states. Nucleation of the metallic phase was observed, as seen in Figure 7, in the samples subjected to more than a 30-pct reduction level, which was about 6 minutes of reduction time. Stoichiometric calculations showed that in order to completely reduce Mn^{3+} to Mn^{2+} and Fe^{3+} to Fe^{2+}, about 33-pct reduction level was required, which is in very good agreement with experimental observations. Therefore, it can firmly be concluded that the

Table III. Results of X-Ray Diffraction Analysis of Wessel Manganese Ores

WH Ore		W1 Ore		W4 Ore	
Mineral	Composition	Mineral	Composition	Mineral	Composition
Braunite II	$Ca_{0.5}(Mn, Fe)_7\ Si_{0.5}O_{12}$	Bixbyite	$(Mn, Fe)_2O_3$	Braunite II	$Ca_{0.5}(Mn, Fe)_7SiO_{12}$
Hausmannite	Mn_3O_4	Manganite	γ-MnOOH	Hausmannite	Mn_3O_4
Hematite	Fe_2O_3	Hausmannite	Mn_3O_4	Hematite	Fe_2O_3
Manganite	γ-MnOOH	Hematite	Fe_2O_3	Calcite	$CaCO_3$
Calcite	$CaCO_3$	Calcite	$CaCO_3$	Androdite (trace)	$Ca_3Fe_2SiO_{12}$

Table IV. Major Phases Detected by X-Ray Analysis in W4 Manganese Ore Samples Exposed to Increasing Extents of Reduction at 1300 °C

Reduction Time (Min)	Reduction (Pct)	Phases Detected*
2	10.68	graphite, MnO, Mn_3O_4, Fe_3O_4
6	44.84	graphite, MnO, α-Fe, Mn_3O_4, Fe_3O_4, $MnFe_2O_4$
8	53.65	graphite, MnO, α-Fe
20	63.60	graphite, Fe-Mn carbide, MnO, silicate slag
30	66.87	graphite, Fe-Mn carbide, MnO, silicate slag
50	81.73	graphite, Fe-Mn carbide, MnO, silicate slag
70	84.62	graphite, Fe-Mn carbide, silicate slag
100	87.21	graphite, Mn-Fe carbide, silicate slag
120	87.94	graphite, Mn-Fe carbide, silicate slag

*Phases detected are listed in order of decreasing intensity of diffraction peaks.

first stage of reduction involved reduction of the higher manganese and iron oxides to their lower states. Thereafter, metallization started with nucleation of iron from wustite. Energy-dispersive X-ray analysis and electron microprobe analysis (EMPA) showed that the metallic nuclei were practically pure iron (about 96 pct Fe) with very low proportions of manganese. Random nucleation of iron may be attributed to the dispersion of iron oxides throughout the matrix. With an increase in reduction time, carburization of metallic iron occurred possibly by direct contact with carbon. Thereafter, this initial carbide played an important role in the reduction of manganous oxide during the second stage of reduction. The oxide was found to be in the form of rounded grins that consisted of mainly manganous oxide (Figure 7). With increasing retention times, growth of small white nuclei that were iron manganese carbides on the edge of grey MnO grains occurred, as seen in Figure 8. The EDAX showed significant increase in the manganese concentration of the metal phase with increasing extent of reduction. Growth of these metal nuclei and the increased amount of silicate phase are shown in Figure 9. As the reduction proceeded, the major phases were mixed carbide of iron and manganese; manganous oxide; and a Ca-Mn silicate phase formed possibly as a result of the reaction between manganous oxide, calcium oxide, and silica. The EDAX showed that the silicate phase formed at a temperature of 1200 °C or higher, consisted mainly of MnO, CaO, and SiO_2. The average composition of the silicate phase formed is approximately $(Ca, Mn)_2SiO_4$. This composition shifted toward the Ca_2SiO_4 phase as reduction proceeded, confirming X-ray results.

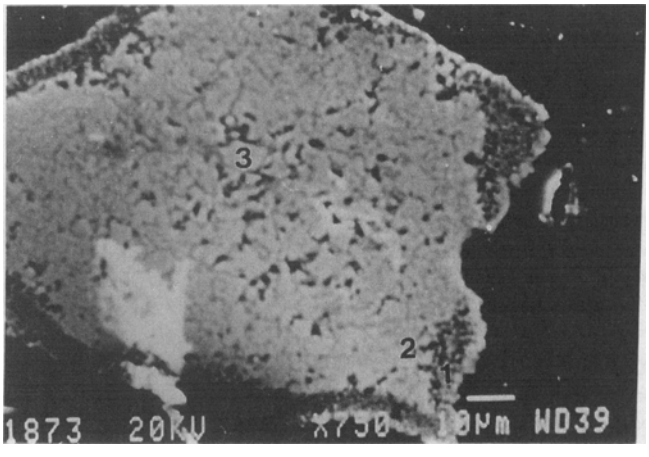

Fig. 6—Wessel: WH, manganese ore grain subjected to a 17.12-pct reduction for 4 min at 1300 °C under argon atmosphere. SEM magnification times 450.

Results of Quantitative Analyses by EDAX

Point	Mn Pct	Fe Pct	Ca Pct	Si Pct	Mg Pct
1	49.90	5.52	2.54	5.31	0.00
2	65.87	9.20	1.74	3.06	0.15
3	71.80	9.58	0.15	0.17	0.12

IV. THE REDUCTION MECHANISM

A. *First Stage of the Reduction*

At all temperatures studied, this stage of the reduction was completed within the first 6 to 10 minutes of retention times. It is expected that reduction originally starts with the following reactions through direct contact between ore and graphite particles:

$$3Mn_2O_3 + C = 2Mn_3O_4 + CO \quad [4]$$

$$3Fe_2O_3 + C = 2Fe_3O_4 + CO \quad [5]$$

These reactions form carbon monoxide, which act as a reducing agent in addition to graphite:

$$Fe_3O_4 + CO = 3FeO + CO_2 \quad [6]$$

$$Mn_3O_4 + CO = 3MnO + CO_2 \quad [7]$$

The CO_2 is reduced back to CO through Reaction [1] by the excess carbon present in the system. It is assumed that reduction of Fe_2O_3 to Fe_3O_4 and Mn_2O_3 to Mn_3O_4 occur instantaneously and that Reaction [6] is fast enough not to contribute to rate control. During this stage, reaction products are porous (Figure 6). The average porosity of the oxide product layer were found as 16.4 pct, 11.2 pct and 20.5 pct for WH, W1, and W4 ores, respectively, by the use of an image analyzer.

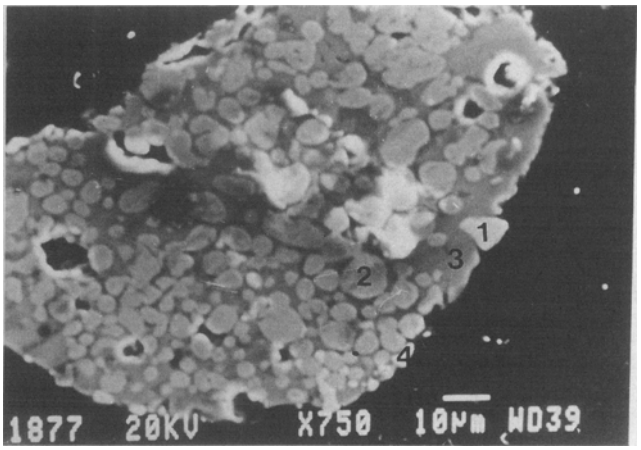

Fig. 7—Wessel: WH, manganese ore grain subjected to a 33.87-pct reduction for 8 min at 1300 °C under argon atmosphere. SEM magnification times 750.

Element Concentrations Determined by EDAX

Point	Mn Pct	Fe Pct	Ca Pct	Si Pct	Mg Pct	Possible Phase
1	1.98	96.93	0.26	0.06	0.04	Fe-rich metal
2	74.78	2.35	0.56	0.10	0.47	MnO
3	36.25	3.69	5.28	11.87	0.74	silicate phase
4	0.69	95.15	0.09	0.04	0.04	Fe-rich metal

B. *Second Stage of the Reduction*

Metallic iron forms as a result of the following reaction:

$$FeO + CO = Fe\ (nuclei) + CO_2 \qquad [8]$$

Thus, second stage, which was virtually absent at temperatures at or below 1200 °C, starts with random nucleation of iron metal from wustite, both in the interior of the particles as well as on the surfaces exposed to the reducing agent. This random nucleation of iron may be attributed to the dispersion of iron oxides throughout the ore matrix. Formation of cracks and imperfections in the ore particles is very likely as a result of the reactions occurring during the first stage of reduction, which, in addition to those originally present, may be considered as the most active sites for nucleation during early periods of the second stage. The metallic iron that is formed is an intermediate product and transforms into iron carbide as reduction proceeds. Thereafter, the iron carbide may act as a medium through which the carbon diffuses to the metal oxide-carbide interface, where more oxide is reduced. Figures 8 and 9 show that with an increase in retention time, an increase in the size of nuclei was accompanied by a significant increase in their manganese content, which is an indication of reduction of MnO-rich oxide grains, which are in contact with iron-rich mixed carbide. The EDAX showed that the mixed carbide was progressively enriched in Mn during this stage (Figures 8 and 9), while at the same time, a Ca-Mn silicate slag formed and spread as a result of the reaction between manganese oxide, lime, and silica. Once the metallic phase starts covering the oxide phase, the reaction of oxide with carbide becomes dominant. The reduction of MnO may then be represented by the reaction

$$MnO + (C)_{metal} = (Mn)_{metal} + CO \qquad [9]$$

The composition of the carbide phases formed (obtained by EDAX) at different retention times above 1200 °C

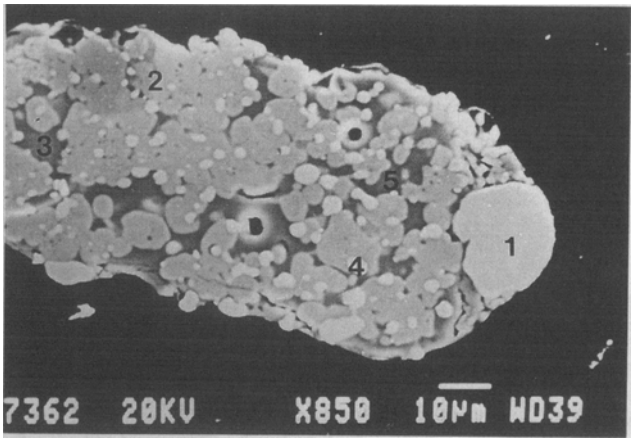

Fig. 8—Wessel: W1, manganese ore grain subjected to a 55.31-pct reduction for 30 min at 1300 °C under argon atmosphere. SEM magnification times 850.

Element Concentrations Determined by Edax

Point	Mn Pct	Fe Pct	Ca Pct	Si Pct	Mg Pct	Possible Phase
1	40.87	52.40	0.53	0.15	0.09	carbide
2	73.05	1.11	1.11	0.24	0.68	carbide
3	36.24	0.59	19.33	12.92	0.55	silicate
4	42.73	53.51	0.43	0.14	0.07	carbide
5	31.38	0.00	19.29	14.32	0.59	silicate

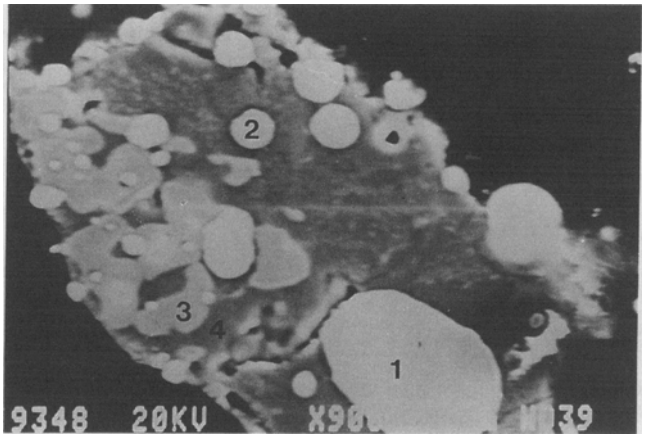

Fig. 9—Wessel: W4, manganese ore grain subjected to a 81.73-pct reduction for 50 min at 1300 °C under argon atmosphere. SEM magnification times 900.

Element Concentrations Determined by EDAX

Point	Mn Pct	Fe Pct	Ca Pct	Si Pct	Mg Pct	Possible Phase
1	55.79	41.68	0.15	0.08	0.00	carbide
2	62.03	33.07	0.24	0.13	0.03	carbide
3	77.08	1.33	1.36	0.22	2.40	MnO
4	14.43	0.26	31.42	14.33	0.66	silicate

were compared with the compositions on the liquidus surface of the Fe-Mn-C system.[35] As the retention time increases, together with increasing manganese content, liquidus temperature of the carbide phase decreases, indicating the existence of a solid-liquid mushy state at temperatures above 1300 °C, which enhances the transport of reactants and products.

With increasing reduction, while the metallic beads increase in size, the proportion of slag also increases. Further reduction of the manganous oxide appears to occur by first dissolution of manganous oxide into the slag and then reduction at the interfaces between the slag and the metal or between the slag and the reducing agent. It is difficult to conclude with certainty whether reduction by carbon dissolved in the metal or the reduction by solid carbon was the dominant reaction. Reduction at the interface between the metal and slag layer would become increasingly important as the amount of solid carbon decreases. There is evidence[36] that the rate of reduction of solid MnO by carbon dissolved in Fe-Mn-C melts is controlled by the rate of the chemical reaction, and it is highly possible that chemical reaction is the rate-controlling process during reduction of MnO dissolved in the slag by the carbon of the metal by the following reaction:

$$MnO_{slag} + C_{metal} = Mn_{metal} + CO \qquad [10]$$

V. THE KINETICS OF REDUCTION

A. *Assessment of Rate Control*

The present experimental data for each manganese ore were initially analyzed by using the chemical control equation outlined in the following:

$$kt = [1 - (1 - F)^{1/3}] \qquad [11]$$

where F is the fraction reacted, k is the rate constant, and t is time.

When this equation was applied to the present data, very good fits were obtained. Correlation coefficients (r) for the chemical control equations to describe the reduction process at temperatures between 1100 °C and 1350 °C were above 0.97, and the calculated activation energies were 87.69 ± 4.8 kJ/kg/mol for W4 ore, 105.08 ± 7.3 kJ/kg/mol for W1 ore, and 114.78 ± 7.2 kJ/kg/mol for WH ore. The plus or minus variations were obtained by testing the data on different particle size ranges of the same ore with the same equations. These small variations can be considered to be within experimental error ranges, and the results indicate that the effects of chemical control are important in the reduction of the Wessel manganese ores.

There are two major rate control processes involved in the topochemical mode of reduction of oxides:[37] (1) diffusion control and (2) mixed control, where both chemical and diffusional processes contribute. For diffusion control, the time (t) for reduction would be proportional to the square of particle size (r_p) and for chemical reaction control, it would be proportional to the first power of r_p. Thus, the variation of the initial rate that corresponds to the first stage of the reduction was plotted against the particle radius in Figure 10. The

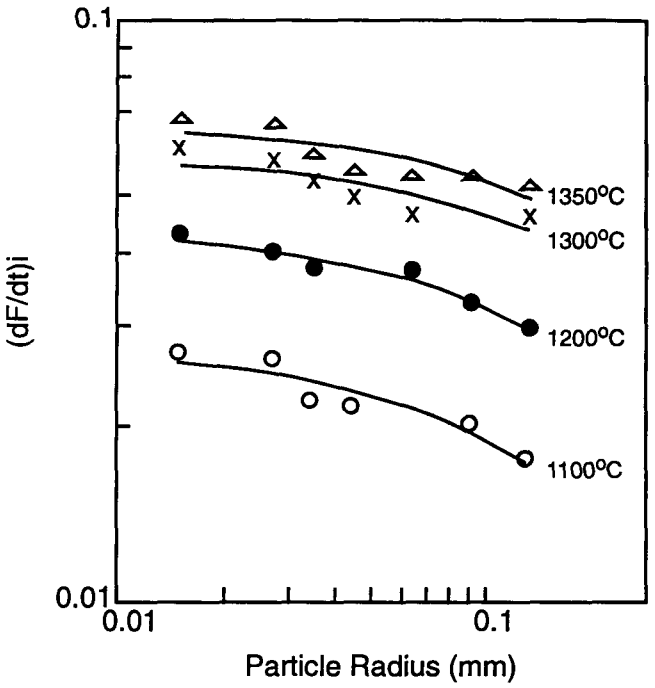

Fig. 10—Initial rate of reduction of WH ore as a function of particle radius at indicated temperatures.

slopes of the curves increase with increasing particle radius, especially for particle sizes greater than approximately 0.02 mm. This behavior suggests the approach to mixed control for the first stage of the reduction. Furthermore, a plot of log $[1 - (1 - F)^{1/3}]$ *vs* log t, as shown in Figure 11, gave slopes from 1.22 to 1.88 for temperatures ranging from 1100 °C to 1350 °C. This is also a clear indication of mixed control for the first stage of reduction, since for sole chemical control the slopes should have been unity.[38] However, for the second stage of the reduction, when the time to achieve a certain percentage of reduction was plotted against particle size

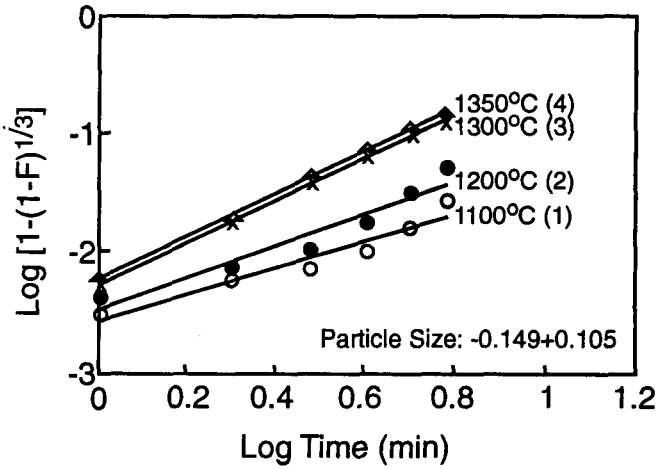

Fig. 11—Log-log plot of the chemical reaction rate-control equation to W1 ore data in the temperature range 1100 °C to 1350 °C. Correlation coefficients, r, for (1) 0.972, (2) 0.972, (3) 0.995, and (4) 0.995. Slopes: (1) 1.22 + 0.14, (2) 1.44 + 0.18, (3) 1.88 + 0.05, and (4) 1.88 + 0.05.

at different temperatures for each manganese ore, straight lines with slopes very close to unity were obtained especially for reduction percentages higher than 65 pct. This was a clear indication that chemical reaction rate control dominated the second stage.[39]

When the logarithm of the experimental initial rates corresponding to the first stage of reduction were plotted with respect to inverse temperature, the activation energies (in the temperature range of 1100 °C to 1350 °C) varied from 81.3 to 94.6 kJ/kg/mol depending on the ore, as shown in Figure 12. Yun[40] reported 62.7 kJ/kg/mol as the activation energy value for reduction of Fe_2O_3 to FeO with carbon by chemical control. For Fe_2O_3 reduction to iron with carbon, an apparent activation energy value of about 133 kJ/kg/mol has also been reported[11] for the chemical reaction rate-controlling mechanism. During MnO_2 reduction to MnO with carbon, Misra[32] reported an apparent activation energy value of 38 kJ/kg/mol and attributed this value to the gaseous diffusion rate-controlling mechanism. It could thus be concluded that the first stage is mainly confined to the reduction of manganese oxides and of hematite to their lower valency states MnO and FeO, and that rate is mixed controlled.

B. *Mathematical Analysis*

For the first stage of the reduction, a mathematical analysis that depicts collectively the chemical reaction on the pore walls of the oxide and the gas diffusion in porous oxide was developed. Because of the porous nature of the product layer during this stage, the total pressure within the sphere is assumed to be constant and essentially the same as that in the gas stream. The mathematical analysis is for a binary gas mixture of CO-CO_2 for which the diffusivity is independent of gas composition, and the effective diffusivities of CO and CO_2 are equal. Furthermore, because of the relatively high thermal conductivity of the metal oxides, heat transfer was dismissed as a possible rate-controlling process. With these justified simplifications, the mathematical formulation is based on the following assumptions: (1) The reaction on the pore walls of oxide is accompanied by gas diffusion, depending on the porosity and gas diffusivity therein. There will be partial internal reduction slightly ahead of nominal product/oxide interface. (2) A quasi-stationary assumption is made for a first-order-type reaction involving CO and CO_2 in a spherical porous particle. (3) The resistance to the film diffusion around the particle is negligibly small. (4) Isothermal and isobaric conditions exist. The mathematical development for this stage is very complex and involved, and it is beyond the scope of this article. However, it is based on the principles given by Ishida and Wen,[38] and thus, details can be found in their article.

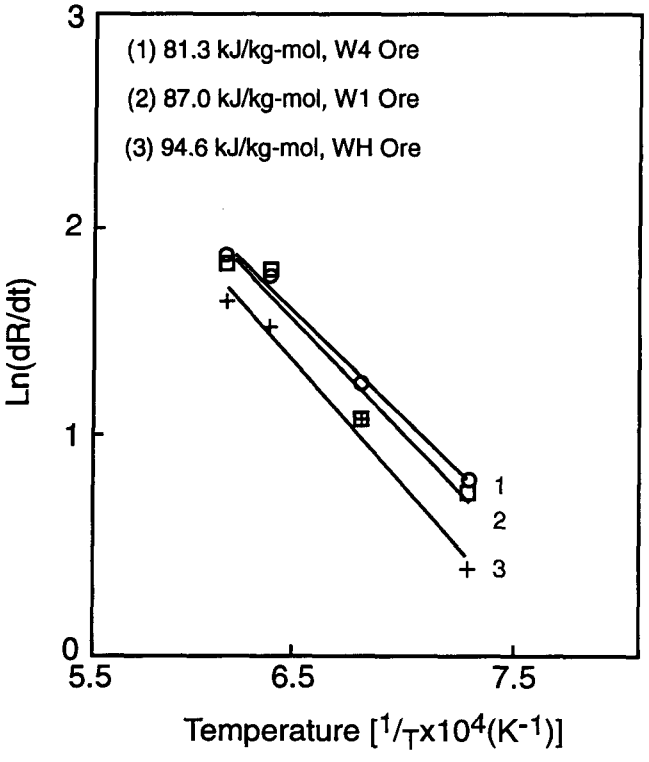

Fig. 12—Determination of apparent activation energy for the first stage of reduction (R is percent reduction).

At the end of the first stage, the fractional conversion is given by the following equation:

$$F_f = 3\,\frac{(\phi_f \coth \phi_f - 1)}{\phi_f^2} \qquad [12]$$

where ϕ_f is the kinetic-diffusion parameter known as the Thiele[42] modulus. It is frequently used to show the effect of gas diffusion on the reaction rates on catalyst pore walls and is defined as

$$\phi_f = \left(\frac{S\rho k(1 + K_e)}{D_{ef}K_e}\right)^{1/2} r_p \qquad [13]$$

where K_e is the equilibrium constant (for reduction Reaction [7]), D_{ef} is the effective CO-CO_2 diffusivity, S is the pore surface area, k is the rate constant, r_p is the initial particle radius, and ρ is the density of particle.

The values of effective CO-CO_2 diffusivities generated by the model (Eq. [13]) were 2.15×10^{-5}, 5.10×10^{-5}, and 6.17×10^{-5} $cm^2 \cdot s^{-1}$ for WH, W1, and W4 ores, respectively, at 1300 °C, several orders of magnitude lower than the intermolecular diffusivities (5.07×10^{-3}, 2.36×10^{-3}, and 7.99×10^{-3} $cm^2 \cdot s^{-1}$ for WH, W1, and W4 ores, respectively) calculated by using the theoretical equations based on the kinetic theory and Lennard–Jones expression for intermolecular forces.[44] It is well known that in porous media the diffusive flux may occur *via* either molecular diffusion or Knudsen diffusion. Because the effective diffusivity values generated by the model are much lower than the molecular diffusivity values, it can be assumed that in this case, Knudsen diffusion is the predominant mode of diffusion. The value of the Knudsen diffusivity calculated for the present study using the equation provided by Satterfield and Sherwood[43] is 6.66×10^{-5} $cm^2 \cdot sc^{-1}$ at 1300 °C, which is found to be in reasonably good agreement with the value of 3.03×10^{-4} $cm^2 \cdot s^{-1}$ for the Knudsen diffusivity calculated by Grimsley[31] from the reduction data of Mamatwan manganese ore at 1300 °C. Grimsely also calculated the effective CO-CO_2

diffusivities that were in the range from 7.9×10^{-5} to 1.59×10^{-4} $cm^2 \cdot s^{-1}$. He attributed these values to the major role played by Knudsen diffusion. By using the effective diffusivities generated by the model, the values of Thiele modulus, ϕ_f, were calculated for different particle sizes for the first stage of the reduction that was found to increase with increasing particle size. This shows that the mixed (diffusion-reaction) rate control in the first stage of reduction is confined to the pore mouths at the outer surface of the particles. When ϕ_f is small, at small particle sizes, there is rapid gas diffusion, and hence, uniform internal reduction occurs throughout the oxide particle, which was confirmed by the calculated effective diffusivities of CO in CO/CO_2 mixtures.

During the second stage, a clear interface develops between the metallic phase containing iron and manganese carbides and manganous oxide. The chemical reaction between the manganous oxide and the carbon dissolved in the metal phase or with the metal carbide seems to be the rate-controlling process. The reaction is localized at the interface between manganous oxide and mixed carbide of iron and manganese, which is evident from the photomicrographs taken from the second stage of the reduction. In order to test the validity of this assumption, a given set of observations of fraction reacted (F) of manganese ores were tested for linearity by plotting $[1 - (1 - F)^{1/3}]$ vs time. From these graphs, rate constants were calculated and used in an Arhenius plot to calculate the activation energy. The calculated activation energies for the second stage of the reduction changed from about 102.1 kJ/kg/mol for W4 ore to 141.7 kJ/kg/mol for WH ore with correlation coefficients above 0.98 (Figure 13). These activation energy figures were well in the range of chemical reaction–controlled regimes, suggesting that during the second stage, the chemical control is predominant.

The model prediction of reduction percentages during the second stage of the reduction, F_s, can be found from the following equation used by King and Brown[44] for impervious core reactions:

$$F_s = 1 + \delta_s^3 F_f - \delta_s^3 \qquad [14]$$

where F_f is the fractional conversion at the end of the first stage. In order to determine F_s, the dimensionless radius during the second stage of the reduction given by Eq. [15] must be calculated:

$$\delta_s = 1 - \frac{R_s}{3C_{so}r_p}(t - t_f) \qquad [15]$$

where R_s is the rate of reduction during the second stage, t_f is the time taken to complete the first stage, and C_{so} is the initial concentration of solid reactant. Equation [15] gives the position of the outer interface during the second stage at time (t). In order to determine δ_s, certain key parameters such as time to complete conversion (t_{tot}) and dimensionless time taken for complete conversion of MnO as a shrinking core (θ_r) had to be estimated by using the experimental data of the reduction during the second stage. The time required for the reaction to complete both the first stage and the second stage, t_{tot}, can be found from Eq. [16].

$$t_{tot} = t_f + \frac{3C_{so}r_p}{R_s} \qquad [16]$$

A dimensionless ratio of the time to complete the first stage to the time taken for complete reduction of MnO as a shrinking core (θ_r) can be defined as[44]

$$\theta_r = \frac{3C_g k S \rho r_p}{R_s} \qquad [17]$$

where C_g is total gas concentration.

The time to complete conversion was estimated by using the experimental values. The t_f was taken as 6 minutes. The R_s values changed between 1.53×10^{-5} and 1.32×10^{-7} $mol \cdot s^{-1} \cdot cm^{-2}$ for WH ore and W4 ore, respectively. The value for W1 ore was in between these two. Specific rate constants for the second stage of the reduction (k_s) values varied from 3×10^{-7} to 2.6×10^{-6} cm/s, which are much smaller than specific rate constants for the first stage of the reduction (k_f), which were in the range between 3.9×10^{-4} and 1.1×10^{-3} cm/s, due to the fact that the rate of the second stage of the reduction is much slower than the rate of the first stage.

The estimated R_s values were then used in Eq. [16] from which the time to complete conversion can be predicted. These values were later inserted in Eqs. [17] and [15] to predict the parameters θ_r and δ_s, which were used to calculate the values for F_s. The application of model by using Eqs. [12] and [14] to the experimental data can be demonstrated by studying the nature of the plots of reduction *vs* dimensionless time. These plots are given in Figures 14 through 16, together with the plot of reduction percent *vs* dimensionless time determined by the TGA setup. A closer examination of the plots reveals that in the first stage of reduction between 0- and 35-pct reduction level, there is a slight difference between experimental and predicted curves that is probably due to inadequacy of the assumptions that the effective diffusivities of CO and CO_2 are equal and also constant at a given temperature. In addition to these in the definition of kinetic-diffusion modulus (ϕ_f), the pores are assumed to be uniform in cross sections, and the surface area remains unchanged throughout the process. These assumptions may have caused the small discrepancies between the model prediction and experimental data.

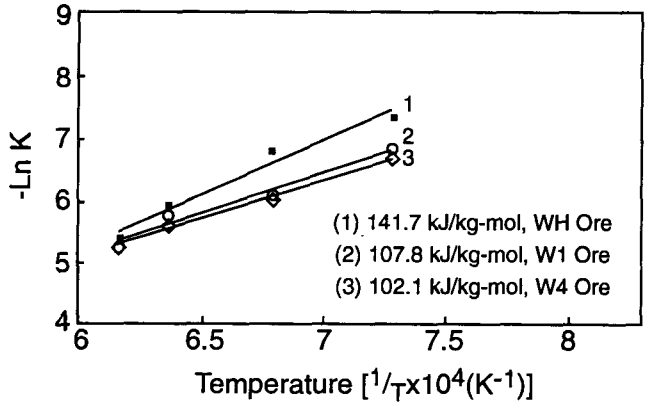

Fig. 13—Determination of apparent activation energy for the second stage of the reduction.

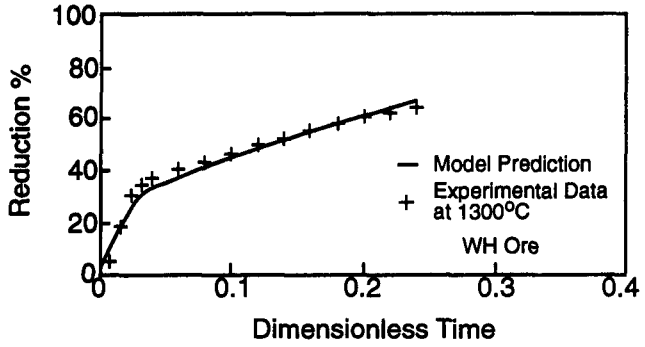

Fig. 14—Model prediction compared with the experimental data for particle size −0.105 + 0.074 mm at 1300 °C with θ_r = 40 and ϕ_f = 8.9.

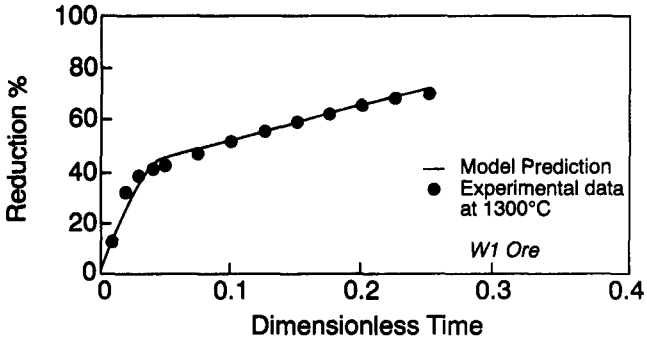

Fig. 15—Model prediction compared with experimental data for particle size −0.074 + 0.063 mm at 1300 °C with θ_r = 25 and ϕ_f = 6.6.

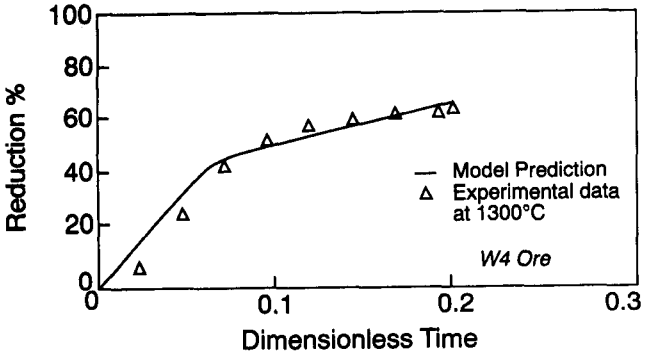

Fig. 16—Model prediction compared with experimental data for particle size −0.210 + 0.149 mm at 1300 °C with θ_r = 15 and ϕ_f = 5.6.

VI. SUMMARY AND CONCLUSIONS

The rate and degree of reduction of the WH, W1, and W4 type Wessel manganese ores were found to increase with increasing temperature and decreasing particle sizes of both ore and graphite, markedly, at temperatures 1300 °C and 1350 °C under argon atmosphere. The effect of chemical composition of the manganese ores on the reduction degree and the rate has also been studied. Results showed that the reduction rate increased with decreasing the Mn:Fe ratio of the ore and increasing the Fe_2O_3 content. The reduction process was found to occur in two distinct stages. For these two stages, a detailed kinetic model is developed, taking into account the chemical and diffusional factors affecting the process. The rate control in the first stage is mixed. The inward diffusion of CO and outward diffusion of CO_2 across the porous product layer and the rate of chemical reaction between CO and solid oxide on the pore walls influenced the overall rate. For the first stage, the mathematical treatment gave the values of effective CO-CO_2 diffusivities as 2.15×10^{-5}, 5.10×10^{-5}, and 6.17×10^{-5} $cm^2 \cdot s^{-1}$ for WH, W1, and W4 ores, respectively, at 1300 °C. It was shown that Knudsen diffusion dominated the gas transport mechanism. As reduction proceeds, relative contribution of chemical resistance increases while that of the diffusional resistance decreases. Apparent activation energies calculated from the reduction rate data corresponding to the first stage of the reduction were 81.3, 87.0, and 94.6 kJ/kg/mol for W4, W1, and WH ores, respectively. After about 6 minutes, the second slower stage starts with nucleation of iron from wustite. The chemical reaction between manganous oxide and carbon dissolved in the metal or metal carbide seemed to be the rate-controlling process. The rate of chemical reaction between MnO and carbide was found to lie in the range from 1.53×10^{-8} to 1.32×10^{-7} $mol \cdot s^{-1} \cdot cm^{-2}$. Apparent activation energies calculated were 102.1, 107.8, and 141.7 kJ/kg/mol for W4, W1, and WH ores, respectively. During this stage, the reaction is localized at the oxide/carbide interface and proceeds as a shrinking core. A calcium silicate phase containing some manganese dissolved in it also forms. It is possible that manganese is also reduced from this silicate phase.

ACKNOWLEDGMENTS

The authors are grateful to the Council for Mineral Technology (Mintek) and Ferro Alloy Producers Association of South Africa for providing funds to conduct this research.

REFERENCES

1. F.R. Morral: *CIM Bull.*, 1984, vol. 77 (86), pp. 72-75.
2. A.S.E. Kelyenstuber: *Proc. 12th CMMI Congress, S. Afr. Inst. Min. Metall.*, Johannesburg, 1980, pp. 213-20.
3. V.N. Misra and P.R. Khangaoukar: *J. Inst. Eng. (India)*, 1975, vol. 55MM (283), pp. 59-63.
4. W. Hofmann, T. Vlajcic, and G. Rath: *Proc. Infacon 89*, New Orleans, LA, The Ferroalloys Association of the United States, Arlington, VA, 1989, vol. 1, pp. 185-95.
5. R.H. Tien and E.T. Turkdogan: *Metall. Trans. B*, 1977, vol. 8B, pp. 305-13.
6. Y.K. Rao: *Metall. Trans.*, 1971, vol. 2, pp. 1439-47.
7. Y. Maru, Y. Kuramasu, U. Awakura, and Y. Kondo: *Metall. Trans. B*, 1973, vol. 4B, pp. 2591-98.
8. N.S.S. Murti and V. Seshadri: *Trans. Iron Steel Inst. Jpn.*, 1982, vol. 22, pp. 925-33.
9. A.K. Biswas: *Principles of Blast Furnace Iron Making Theory and Practice*, Cootha Publishing House, Brisbane, Australia, 1981.
10. E.T. Turkdogan, V. Koump, J.V. Vinters, and J.F. Perzak: *Carbon*, 1968, vol. 6, pp. 467-84.
11. E.A. Gulbransen, K.F. Andrew, and F.A. Brassort: *Carbon*, 1965, vol. 2, p. 421.

12. E.T. Turkdogan and J.V. Vinters: *Carbon*, 1970, vol. 8, pp. 39-53.
13. E.T. Turkdogan and J.V. Vinters: *Metall. Trans.*, 1972, vol. 3, pp. 1561-74.
14. G. Heynert and J. Willems: *Stahl. u. Eisen*, 1959, vol. 79, pp. 1545-54.
15. S. Ergun: *Phys. Chem.*, 1966, vol. 60, p. 480.
16. M. Rossberg: *Z. Elektrochem.*, 1956, vol. 60, p. 952.
17. P.L. Walker, Jr., F. Rusinko, Jr., and L.G. Austin: *Advances in Catalysis*, Academic Press, New York, NY, 1959, vol. 11, pp. 133-321.
18. A.F. Armington: Ph.D. Thesis, Pennsylvania State University, University Park, PA, 1960.
19. G.J.W. Kor: *Metall. Trans. B*, 1978, vol. 9B, pp. 307-11.
20. B.E. Hunt, S. Mori, S. Katz, and R.E. Beck: *Ind. Eng. Chem.*, 1953, vol. 45, pp. 677-80.
21. A. Pahme and H.J. Junker: *Brennst. Chem.*, 1955, vol. 36, pp. 193-99.
22. K. Hedden: *Brennst. Chem.*, 1960, vol. 41, pp. 193-99.
23. K. Tereyama and M. Ikeda: *Trans. Jpn. Inst. Met.*, 1985, vol. 26 (2), pp. 108-14.
24. W.J. Rankin and J.S.J. Van Deventer: *J.S. Afr. Inst. Min. Metall.*, 1980, vol. 80 (7), pp. 239-47.
25. A. Koursaris, A.S.E. Kleyenstuber, and C.W.P. Finn: *Spec. Publ. Geol. Soc. S. Afr.*, 1983, vol. 7, pp. 375-82.
26. K. Dewar and J.B. See: Report No. 1968, National Institute for Metallurgy, Randburg, South Africa, 1978.
27. V.K. Antonov and G.I. Chyfarov: *Akad. Nauk. USSR Uralskii filial, Tr. Inst. Metall.*, 1961, vol. 7, pp. 101-05.
28. L.M. Tsylev: *The Smelting of Ferroalloys in the Blast Furnace Using Oxygen Enriched Blast* (Polish), Translated by C.M. Burnell, Pergamon Press, Oxford, 1963, vol. 1.
29. H. Van Hien and D.I. Ryzhonkov: *Steel USSR*, 1972, vol. 2, pp. 178-80.
30. A.K. Ashin and S.T. Rostovchev: *Izv. Vyssh. Zaved., Chem. Met.*, 1964, vol. 7, pp. 10-18.
31. W.D. Grimsely: Master's Thesis, University of the Witwatersrand, Johannesburg, 1977.
32. V.N. Misra: *Proc. 14th CMMI Congress*, Edinburgh, 1990, pp. 39-47.
33. R.H. Eric and E. Burucu: *Miner. Eng.*, 1992, vol. 5 (7), pp. 795-815.
34. J.H. Downing: *Elect. Furnace Proc.*, 1963, vol. 21, pp. 288-96.
35. L.N. Barmin: *Fiz. Khim. Osn. Proizvod. Stali.*, 1968, pp. 406-11.
36. E.T. Turkdogan and J.V. Vinters: *Metall. Trans.*, 1971, vol. 2, pp. 3175-88.
37. M. Ishida and C.Y. Wen: *AIChE J.*, 1968, vol. 14 (2), pp. 311-17.
38. O. Levenspiel: *Chemical Reaction Engineering*, Wiley, New York, NY, 1962, pp. 338-57.
39. T.S. Yun: *Trans. Am. Soc. Met.*, 1961, vol. 54, pp. 129-42.
40. J.S.J. Van Deventer and P.R. Visser: *Thermochim. Acta*, 1987, vol. 111, pp. 89-102.
41. E.W. Thiele: *Ind. Eng. Chem.*, 1939, vol. 31, pp. 916-20.
42. C.N. Satterfield and T.K. Sherwood: *The Role of Diffusion in Catalysis*, Addison-Wesley, New York, NY, 1963, pp. 5-16.
43. R.P. King and C.P. Brown: *Metall. Trans. B*, 1980, vol. 11B, pp. 585-92.